

Review of Seeing Like A City By Ash Amin And Nigel Thrift

Original

Review of Seeing Like A City By Ash Amin And Nigel Thrift / Lancione, Michele. - In: ENVIRONMENT AND PLANNING D-SOCIETY & SPACE. - ISSN 0263-7758. - (2017).

Availability:

This version is available at: 11583/2886863 since: 2021-04-09T08:35:33Z

Publisher:

Sage

Published

DOI:

Terms of use:

This article is made available under terms and conditions as specified in the corresponding bibliographic description in the repository

Publisher copyright

(Article begins on next page)

Pattern-Reversal Visual Evoked Potential on Smart Glasses

Rossana Terracciano, *Student Member, IEEE*, Alessandro Sanginario, Simona Barbero, Davide Putignano, Lorenzo Canavese and Danilo Demarchi, *Senior Member, IEEE*

Abstract—Objective: this work presents an integrated device, based on smart glasses, for the pattern reversal visual evoked potential (PR-VEP) clinical test. **Methods:** smart glasses are used to generate the checkerboard changing pattern, with its related red fixation point through an Android® application. Electroencephalographic signals, for monitoring the stimulus generated by PR-VEP, were amplified close to the scalp and then transmitted wirelessly to a PC. A Matlab® real-time algorithm processed the incoming signals to extract the final PR-VEP signal. **Methods:** 40 eyes (from 20 subjects, 12 males and 8 females between 24–28 years old) were tested and results were compared, with a commercial device for VEP clinical exam, to test the reproducibility and the efficacy of the proposed solution. **Results:** PR-VEPs generated by smart glasses showed typical triphasic waveforms: we observed promising results and components in moderate agreement with those obtained using commercial PR-VEP recorder, with potential for improvements after further refinement works. **Significance:** proposed device leads the way for a portable and low cost solution.

Index Terms—Visual Evoked Potentials, Android, Smart Glasses, Wearable, Integrated Medical Devices

I. INTRODUCTION

Visual evoked potentials (VEPs) are an important means for obtaining reproducible and quantitative data on the function of the anterior and posterior visual pathways [1]. VEP waveforms are electrical potentials, caused by repetitive visual stimuli, which are recorded from the scalp overlying visual cortex [2] and extracted from the electroencephalogram (EEG) by means of signal averaging [3].

VEP tests are especially helpful to identify some pathologies, not easily visible through traditional diagnostic tests [4], that impair the visual pathways in any of its segments [5]. Therefore, they have been shown to be useful for many paradigms in cognitive studies (visual attention, working memory [6], binocular rivalry [7], brain rhythms [8]) and clinical neuroscience (aging [9], neurodegenerative disorders [10], schizophrenia [11], optic pathway pathology [12], migraine [13], autism [14], depression [15], anxiety, stress [16], and epilepsy [17]). Recently, in engineering, SSVEPs (steady state visually evoked potentials) found a novel application for SSVEP-driven braincomputer interface (BCI) systems [18].

Several types of stimuli can elicit VEPs [19], but the most widely used in clinical practice are flash and pattern stimulations [20]. A flash VEP is obtained when a uniform flash is

used as stimulus [21], while pattern stimulation corresponds to the use of reversal of a stimulus (usually a checkerboard or alternating bars) [20].

Flash-VEPs (morphological model is shown in Figure 1a) consist of a series of negative and positive waves; the most predominant are the N2 (90 ms) and P2 (120 ms) peaks [20] of the detected electroencephalographic signal.

They are extremely variable across different subjects with respect to pattern responses but show less interocular asymmetry [22]. In Figure 1b is depicted the morphological model of a pattern reversal VEP signal (PR-VEP). It consists of a prominent negative component after a time of about 75 ms (N75) after signal start, a larger amplitude positive component at about 100 ms (P100) and a more variable negative component at about 135 ms (N135) [20]. PR-VEPs have the lowest variability in waveform and peak latency across different subjects [23].

Even though PR-VEPs have been used in clinical and research laboratories for more than 40 years since Halliday et al. pioneering work in the early 1970s [24], visual stimuli are still presented on cathode ray tube (CRT) monitor, plasma displays and, in recent years, on LCD displays, such as consumer television or PC monitors, despite some concerns [25], [26]. Such displays need to be calibrated especially in their contrast ratio and luminance [27].

The major issues of this equipment are the large size of the visual stimulator [28] (sometimes screens larger than 40 inches) and the high cost of the devices due to the expensive apparatus (amplifier and AD board) [29]. Therefore the wide space required (usually hospitals or clinics use a room exclusively for this type of exam) and the expensiveness pieces of equipment are drawbacks that have hindered the introduction of PR-VEPs into routine clinical practice. As a matter of fact, these factors practically make impossible to execute the exam outside the clinics or hospitals.

In 2016 a pilot study was conducted comparing a new PR-VEP stimulation method, based on the use of a head-mounted display (HMD), with the conventional CRT-based stimulator with good results [30]. In that work they used the head mounted-OLED microdisplays SVGA-connected to a personal computer which generated the stimulation pattern and recorded PR-VEPs with a commercial device. In this paper we propose a novel integrate solution to elicit PR-VEP responses by means of smart-glasses with an Android™ application. PR-VEP signals will be recorded with a low-cost electronics and will be sent wirelessly to the physician PC. To be an acceptable alternative to standard PR-VEP exam equipment, a new device

R. Terracciano, A. Sanginario and D. Demarchi are with the Department of Electronics and Telecommunications, Politecnico di Torino - Torino, Italy. D. Putignano, S. Barbero and L. Canavese are with Service of Neuro-Ophthalmology, University of Turin, Turin Ophthalmic Hospital, Torino, Italy. R. Terracciano and A. Sanginario contributed equally to this work.

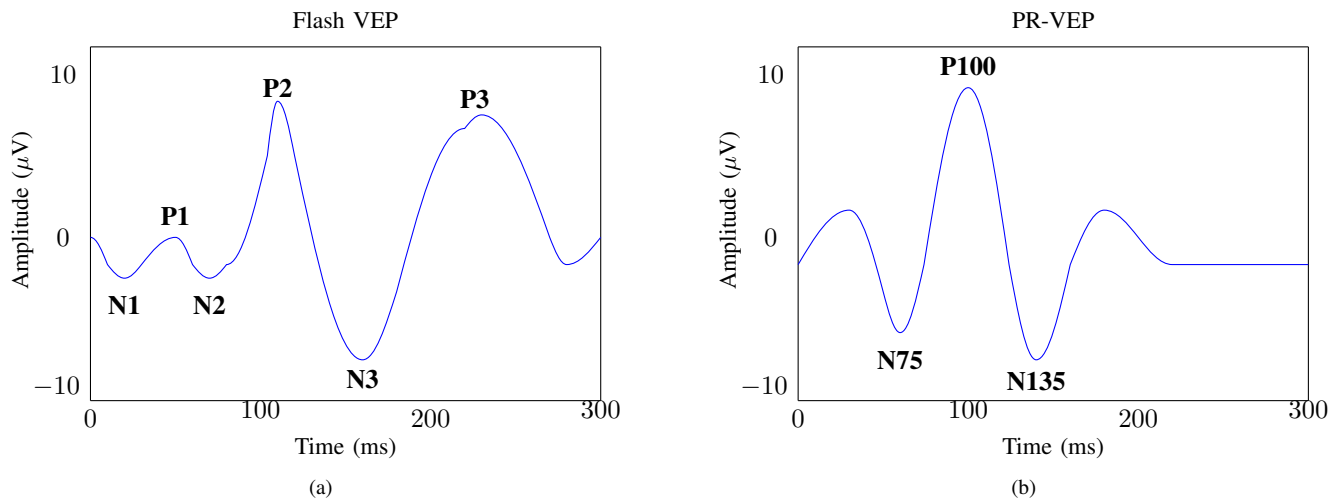


Fig. 1: Typical morphology of the signal flash VEP (a) and pattern-reversal VEP (b), obtained from a healthy subject from our own hospital.

should elicits clear PR-VEP responses in their fundamental components (N75, P100, N135). For this reason, our approach was compared with a commercial device for PR-VEP exam (Figure 2).

The main contribution of this paper is the implementation of a new integrated device with performances comparable with available commercial instruments, but *low cost, portable* and useful for subjects with physical inability to maintain the upright position or the concentration to the visual fixation.

The remainder of this paper is organized as follows: Section II describes the proposed PR-VEP recorder prototype and the details of the performed clinical trial. Experimental setup and performance of our system, in terms of obtained results, are presented in Section III. Finally, in Section IV, we conclude the paper evaluating proposed solution pro, cons and future works.

II. METHODS

A. Instrumentation

PR-VEP testing was performed in *Sperino Ophthalmic Hospital* in Turin, using as a gold standard VEP recorder the commercial device *Retimax Advanced*[®] by CSO [31], in order to compare results with our prototype. As stated in [32] *Retimax Advanced*[®] function for visual evoked potential recording follows the ISCEV recommendations.

On the other hand, smart-glasses used to generate the visual stimulus are the *Moverio BT-200*[®] by Epson [33], with a refresh rate of 60Hz and *Android*[™] as the operating system.

To elicit VEP responses the screen that displays the visual stimulus should have a particular value of luminance and contrast as indicated by ISCEV standards [20]. Such values are easily provided by modern LCD screens following some precautions reported in [34], [35], [27]. A cover for the glasses was designed and 3D printed to isolate the viewer from the outside light as shown in Figure 3a.

EEG signal was recorded and sent wirelessly with an *OpenBCI Cyton*[®] board [36] and then PR-VEP waveform was

extracted by a *Matlab*[®] real-time algorithm. The *OpenBCI Cyton*[®] board is an 8-channel neural interface with a 32-bit processor that adopts a *Bluetooth Low Energy (BLE)* communication system, sample rate of 250Hz and *ADS1299* analog to digital converter. A board holder was designed and 3D printed to be worn from the patient's arm and to contain all the electronics (*OpenBCI Cyton*[®] board, battery, and audio-signal amplifier board).

B. Data acquisition

A full-field PR-VEP test was performed using a monocular stimulus on both eyes of each subject, as recommended in [20]. We collected 80 PR-VEP signals from a group composed of 20 people from 24 to 28 years, 12 males and 8 females. Each subject underwent test using smart glasses and *Retimax Advanced*[®] for both eyes (for a total of 4 measures per subject: left eye with *Retimax*, left eye with smart glasses, right eye with *Retimax*, right eye with smart glasses). The orders of presentation were randomized among subjects and among eyes.

Each subject was selected taking into account that no one had a history of ophthalmologic diseases and visual acuity was measured. All the subjects were considered healthy and they was opportunely refracted with glasses or contact lens, when needed. They all provided informed consent after receiving an explanation of study purposes. Table I summarizes the information about the subjects.

Following 10/20 International Sytem [37], PR-VEP recordings were obtained using an active electrode Oz referenced against mid-frontal electrode Fz. Ground electrode was placed at A₂. Gold cup electrodes were used. Electrode impedance was kept below 10 k Ω to reduce possible artifacts [20].

PR-VEP using *Retimax Advanced*[®] was performed seating the participant comfortably in a quiet darkened room 1000 mm from the plasma-TV display. The subject was instructed to fixate the red fixation point with one eye, while the other eye was covered with a patch. Subjects were carefully observed

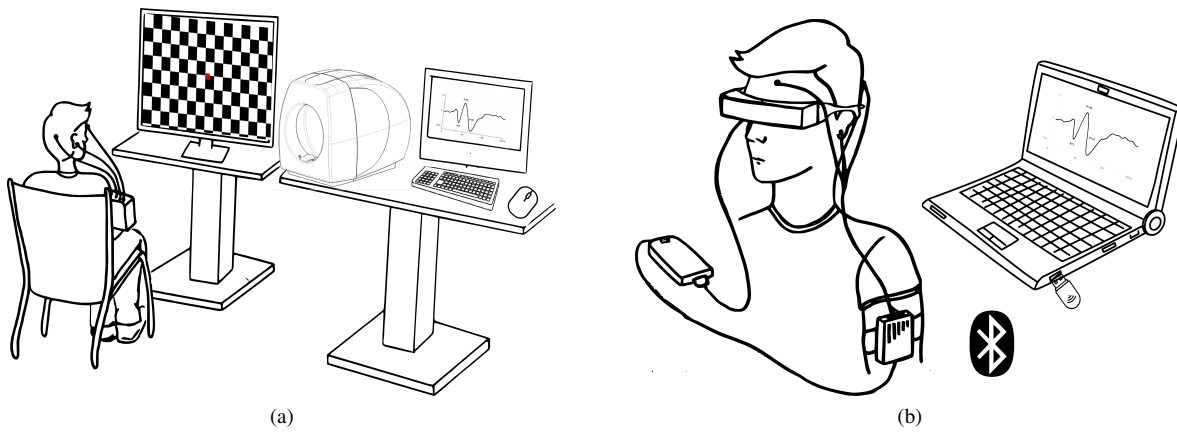


Fig. 2: Comparison between a traditional PR-VEP test (a) and a smart glasses stimulator-based PR-VEP test (b).

TABLE I: Clinical details of the subjects recruited: subject code, gender, age and distance visual acuity (in terms of Monoyer chart) was tested with correction (CC), or without correction (SC). If the correction was a contact lens, CL is used as the identifier.

Subject Code	Gender	Age (Year)	Visual acuity (Left Eye)	Visual acuity (Right Eye)
GDL	Male	24	10/10, SC	10/10, SC
RT	Female	24	10/10, CC, (-2.75D)	10/10, CC (-2.75D)
FR	Male	26	10/10, CL (-1.25D)	10/10, CL (-1.25D)
AM	Male	24	10/10, SC	10/10, SC
DC	Female	26	10/10, CL (-1.75D)	10/10, CL (-1.25D)
SC	Female	24	10/10, SC	10/10, SC
MC	Male	24	10/10, CL (-1.25D)	10/10, CL (-1.25D)
CP	Male	26	10/10, SC	10/10, SC
MCS	Male	24	10/10, SC	10/10, SC
GA	Male	26	10/10, SC	10/10, SC
TL	Female	27	10/10, CC, (-3.25D)	10/10, CC (-3.75D)
MLP	Female	25	10/10, CC, (-2.25D)	10/10, CC (-2.75D)
MR	Male	24	10/10, CC, (-1.25D)	10/10, CC (-1.25D)
MT	Male	25	10/10, CC, (-1.25D)	10/10, CC (-1.25D)
LR	Female	24	10/10, CC (-1.75D)	10/10, CL (-1.25D)
SB	Female	26	10/10, CC (-1.25D)	10/10, CC (-1.25D)
PDF	Female	25	10/10, CL (-2.00D)	10/10, CL (-2.00D)
SM	Male	26	10/10, CL (-1.25D)	10/10, CL (-1.25D)
DP	Male	28	10/10, SC	10/10, SC
AB	Male	25	10/10, SC	10/10, SC

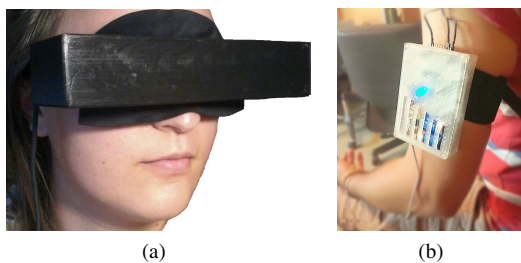


Fig. 3: Two CAD models were developed: the first one was customized from the size of the Moverio BT-200 to isolate the patient from the outside environment (a). The second one was developed to make wearable the acquisition system (b).

during the procedure and urged to keep fixation in case of distraction to ensure adequate fixation.

PR-VEP using our prototype each subject also was performed seating the participant comfortably and adjusting the

smart glasses to produce the clearest image. Also in this case subjects were instructed to fixate the red fixation point at the center of the image with one eye while the other eye was covered with a patch. In order to use the smart glasses Moverio BT-200[®] as a visual evoked potential stimulator, an Android[™] application has been developed. The application lets to set the stimulation parameters (temporal frequency, spatial frequency) before performing the test. Moreover, just like with Retimax Advanced[®] it is possible to obscure half or a quarter of the checkerboard if the purpose is to investigate respectively *hemianopsia* [38] and *quadrantanopia* [39] phenomena.

Parameters set used in our experimental protocol were the same for both systems (Retimax[®] vs Smart Glasses Prototype) and they were the following:

- Pattern shape: reversal checkerboard
- Temporal Frequency: 2 reversal per second (RPS)
- Spatial Frequency: 60 minutes of arc
- Aspect Ratio: 16:9

- Field size: 23°
- Bandpass filter: 1-100 Hz
- Number of epochs averaged: 100
- Sweeps time: 300 ms

Since the frequencies that can be elicited are limited to integer divisors of the monitors refresh rate, the Android™ application was functionalized to deliver the stimulus with a frame-locked reversal frequency. For the clinical trial we used in both Retimax and Smart glasses case a reversal rate of 2.0 ± 0.2 RPS (corresponding to 1.0 ± 0.1 Hz, as written in [20]) and spatial frequency of 60 minute of arc and the contrast was set to 100%. The average response obtained from 100 reversals artifacts-free was analyzed in each acquisition (every subjects was tested at least twice to verify VEPs stability, as ISCEV standard recommends). Ambient light was the same for all recordings and a very low level of brightness was maintained in the room.

Stimulation must be synchronized with the acquisition system: traditionally, the problem of synchronizing the pattern shift instant with the triggering of the recording device is solved by using two ordinary PCs, one for pattern generation and the other for signal recording [40] or using PC with a very fast video processor (and this is the way adopted in Retimax® device). Basically, in our prototype user starts the stimulation directly through the Epson® trackpad: as soon as the smart glasses display the patterned stimulation, a trigger, in the form of a sound impulse, is generated. Through an audio jack and an amplifier circuit, the trigger signal is propagated to a GPIO pin of the OpenBCI Cyton® board. This event starts the EEG recording. Such simple solution is effective in synchronizing the two events as it is shown in the following section.

The extraction of the PR-VEP using smart glasses from the EEG signal was performed by a Matlab® real-time algorithm that implements a 5th order IIR bandpass filter in the 1Hz-100Hz band without any notch filters as ISCEV standards require. Nevertheless, as we are approaching to a new device, we studied the effect of a notch filter in data analysis finding no evident morphology change in the extracted waveforms. Additional details can be found in Supplementary Information document.

According to the ISCEV standards [20], signal was sampled from 0 to 300 ms after stimulus. In order to eliminate blinking artifacts, all epochs with a signal exceeding a threshold of $\pm 35 \mu\text{V}$ are discarded from the average. The number of the discarded is comparable between the two methods, because in both case it is in the range of 0-25 discarded epochs. It wasn't found any dependence from the system used about discarding the epochs. The averaging method is based on the assumption that the noisy EEG activity are uncorrelated with the VEP waveform, thus calculating the average, the noise decreases by a factor of $1/\sqrt{N}$, where N is the number of averaged epochs. The synchronized (time-locked) averaging is essential to separate the buried evoked potential waveforms from other activity [41].

A recurring issue in this kind of experiment is the defocusing in monocular vision into the smart glasses because it could produce an eyestrain during the test. This problem has been partially solved by accustoming for the first time the subject

to the binocular vision into the glasses. In any case, each test was conducted at a very low frequency also to avoid epileptic phenomena.

C. Data processing

Data processing for statistical analysis was performed with Matlab®. For each waveform 10 features regarding triphasic depolarization in terms of latency and amplitude were extracted automatically using a Matlab algorithm that finds peaks (minimum and maximum) in a time range, in which PR-VEP signal is expected, after the stimulus. Another feature extracted is the absolute power density ($\mu\text{V}^2/\text{Hz}$) to retrieve information from the frequency domain analysis (performed using the fast Fourier transform algorithm, with the resolution of 3.33 Hz).

The final goal of this analysis is to compare outputs produced by our prototype with those taken from a commercial device. For this reason, extracted dataset was analyzed to determine the difference in terms of latencies and amplitudes of responses between two different stimuli.

In order to analyze statistically the agreement between the two different stimulators, extracted data were plotted with a Bland-Altman, scatter-plots and boxplots. Finally, Pearson's correlation coefficient was estimated in order to understand if the relationship between the variables is linear or not, and the concordance correlation coefficient was computed for evaluating the reproducibility.

III. RESULTS AND DISCUSSION

Resulting averaged features extracted from the 20 subjects are reported in Table II. Regarding the morphology of the signals, as it is shown in Figure 4, PR-VEP of each stimulus showed typical triphasic waveforms characterized by three dominant peaks of N75, P100, and N135. It is clearly noticeable that the morphology are comparable even though there are some differences in amplitude and latency. PR-VEP amplitudes from Retimax Advanced® were reasonably greater than those from smart glasses. On the other hand, N75, P100 and N135 latencies from Retimax Advanced® were strongly similar to those evoked with smart glasses, but slightly wider than those evoked with smart glasses. No meaningful right to left side difference in latency or amplitude was observed for both methods.

Regarding frequency domain analysis, the PR-VEPs evoked with the Retimax Advanced® seem to provide a higher information content about power density than the smart glasses PR-VEPs. We choose to use also the boxplots to compare and to analyze the features. Supplementary Information document provides a more complete picture of the data and allows to visualize differences among the two methods to evoke visual potentials. Except for the case of the N75 latency in the left eye, the ranges are comparable within the two methods in all the other cases. In fact, very strong similar values of the median are shown in the cases of amplitudes and relative amplitude and P100 latency.

In Figure 5, the correlation between Retimax and smart glasses data and the Bland-Altman plots are reported for the

TABLE II: Features results table: differences between Retimax and smart glasses stimulation in terms of PR-VEP latencies, amplitudes and power. Values are presented as mean \pm standard deviation.

	Left Eye			Right Eye			Right To Left Differences		
	Retimax	Smart Glasses	Absolute Mean difference	Retimax	Smart Glasses	Absolute Mean difference	Retimax	Smart Glasses	Absolute Mean difference
Amplitude (μV)									
N75 Amplitude	-2.05 \pm 1.65	-2.48 \pm 1.27	0.43	-2.54 \pm 1.70	-2.71 \pm 1.26	0.17	0.48 \pm 0.98	0.23 \pm 0.68	0.25
P100 Amplitude	10.99 \pm 2.98	8.67 \pm 3.14	2.31	10.73 \pm 2.75	8.99 \pm 3.18	1.74	1.31 \pm 0.97	0.32 \pm 1.02	0.07
N135 Amplitude	-3.12 \pm 1.95	-3.64 \pm 1.35	0.52	-3.62 \pm 1.45	-3.56 \pm 1.51	0.06	0.50 \pm 0.77	0.07 \pm 0.54	0.42
N75-P100 Amplitude	13.04 \pm 3.88	11.15 \pm 3.72	1.88	13.27 \pm 4.22	11.71 \pm 3.89	1.56	0.23 \pm 1.63	0.55 \pm 1.23	0.32
P100-N135 Amplitude	14.11 \pm 4.16	12.31 \pm 4.19	1.79	14.36 \pm 3.88	12.56 \pm 4.36	1.80	0.32 \pm 1.41	0.24 \pm 1.21	0.01
Latency (ms)									
N75 Time Peak	64.4 \pm 8.59	57.2 \pm 5.96	7.2	68.6 \pm 7.48	58.8 \pm 7.00	9.80	4.2 \pm 8.13	1.60 \pm 6.34	2.6
P100 Time Peak	106.4 \pm 4.18	103.8 \pm 10.73	2.6	106.4 \pm 4.56	104.2 \pm 8.84	2.2	0 \pm 2.39	0.4 \pm 5.94	0.4
N135 Time Peak	167.4 \pm 14.52	164.4 \pm 9.87	3	159.4 \pm 12.60	168.8 \pm 10.43	9.40	8 \pm 12.27	4.4 \pm 7.29	3.6
N75-P100 Time Peak	42 \pm 10.5	46.6 \pm 10.56	64.6	37.8 \pm 10.5	45.4 \pm 9.10	7.6	4.2 \pm 8.63	1.2 \pm 6.16	3
P100-N135 Time Peak	61 \pm 15.78	60.6 \pm 8.63	0.4	53 \pm 10.92	64.6 \pm 10.56	11.60	8 \pm 11.79	4 \pm 7.74	4
Frequency Domain (μV²/Hz)									
Power Density	11.48 \pm 2.68	9.12 \pm 2.36	2.92	11.77 \pm 2.68	9.14 \pm 2.63	1.82	0.70 \pm 0.65	2.25 \pm 1.09	1.55

most significant features: P100 amplitude, P100 latency, and power density. Linear regression analysis allows to evaluate the constant (intercept) and proportional (slope) systematic error: in particular it is possible to notice the presence of a constant systematic error (especially in case of P100 latency component), instead a very slight proportional systematic error (slope is less than 1) is detected.

The Bland-Altman plots were used to easily compare the two measurement systems. In the case of the P100 amplitude, no dependence between the differences and the mean values are noted: the points cluster randomly around the average line of the differences. It is possible to see the presence of a bias (-28% for left eyes, p-value \ll 0.01, and -21% for right eyes, p-value \ll 0.01): 95% of the differences between the two methods is in the range between -86% and 30% for the P100 amplitude of the left eyes and between -83% and 40% for the P100 amplitude of the right eyes.

In the case of the P100 latency feature, smart glasses method produces, on average, lower results than the Retimax method for low latency levels. In this case, the bias is very small (-2.9% for left eyes, p-value $>$ 0.01, and -2.3% for right eyes, p-value $>$ 0.01) and 95% of the differences between the two methods is in the range within -19% and 13%, and -17% and 13% respectively. Such latency differences are still too high for a proper diagnosis instrument. The ways through which they can be reduced are mainly two: from one side it is

necessary to increase the sampling frequency of the acquisition board to obtain a better resolution and to implement the 1-100 Hz band-pass filter with hardware components. On the other hand, a larger set of subjects need to be tested to refine the measurement differences.

Also in the case of the power density, no dependence of the differences are noted from the mean values, as the points cluster randomly around the average line of differences. A small bias (at -27% for left eyes, p-value \ll 0.01, and -24% for right eyes, p-value \ll 0.01) is evident: 95% of the differences between the two methods is in the range between -64% and 11% for the power density of the left eyes and between -55% and 12% for the power density of the right eyes.

Finally, evaluation of the correlation and the agreement between the two techniques is shown in Table III. The most stable component of PR-VEP signal is the P100. The agreement between the two techniques is therefore satisfying (p $<$ 0.05) both in the left eye (respectively CCC=0.55, ICC=0.21, precision=0.71, accuracy=0.77 for the P100 amplitude) and in the right eye (respectively CCC=0.47, ICC=0.13, precision=0.56, accuracy=0.84 for the P100 amplitude). We can affirm that the two systems results have significant congruence according to both methods of comparison (linear regression and Bland-Altman plots). As stated in *International Federation of Clinical Neurophysiology recommendations for visual systems* [42], the physiological properties of the triphasic components of

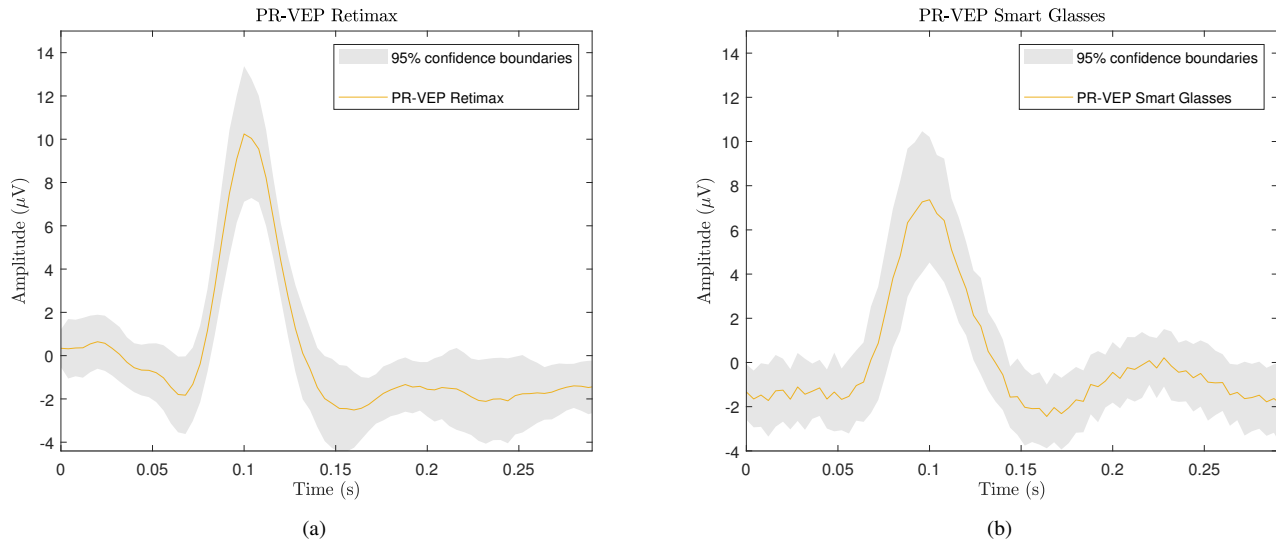


Fig. 4: All the PR-VEP waveforms obtained during the test using: the Retimax stimulator (a) and the smart glasses (b). The PR-VEPs obtained in both cases showed very similar potentials, well-defined in terms of N75, P100, and N135 components.

PR-VEPs differ between subject depending on age, sex and pupil size, affecting both amplitude and latency. For example, females have been shown to have slightly shorter P100 latency, as resulted in [23], and larger P100 amplitude than males. Furthermore, P100 amplitude tends to decrease with a small diameter pupil while the latency of P100 increases. As written in [43], despite the synchronization between the stimulus and the evoked potential, the latency-components are not always constant and can be affected by different kinds of factors, for example, the physiological latency between the stimulus perception and the PR-VEP, sometimes depends on the current cerebral workload (i.e. several tenths of milliseconds). Consequently, it is clear that high jitter values can significantly influence the amplitude of the PR-VEP due to the average. A possible solution, would be the use of realignment algorithm as done in [44], where authors compared latency-jitter correction methods with standard averaging, finding an improved P100 amplitude. It has to be noted though, that such realignment-based method are not supported by ISCEV regulations for standard clinical visual evoked potentials.

In this study was found an electronic jitter of 28 ± 8 ms, deleted automatically before acquisitions. No assumption, instead, was done for the physiological jitter, as the ISCEV regulations state.

IV. CONCLUSION

We proposed an integrated, portable and low cost solution for pattern reversal visual evoked potential tests. The system is able to generate visual stimuli such as (but not limited to) the commonly used checkerboard, with the possibility to choose different parameters (e.g. spatial and/or temporal frequency). The resulting PR-VEPs are acquired synchronously by a commercial EEG acquisition board following the 10/20 International System [37]. Data is then sent to a laptop via bluetooth connection and processed real-time with Matlab®.

Results of our system are compared with a commercial PR-VEPs exam device and show a very strong similarity. Waveforms amplitudes are slight lower in comparison with the Retimax® ones, instead latency differences lies inside a 10% range. These differences are still improvable but they are enough for the purpose of the evaluation of a good propagation of the signal through the optic pathway pathology.

The advantages that derived from our device are several. Its portability can enable PR-VEPs exams at the patient's home. Moreover, the exam could be executed also to bedridden or movement impaired patients but in this regards additional studies may be necessary. Also, the cost of this prototype, considering only the bare components (smart glasses, Cyton board, 3D printed fixture and minor analog electrical components) is less than 1300 EUR. This indicates that the final price in case of commercialization would be sensibly less than the cost of current VEP analysis equipment (around 20000 Euros).

However, several limitations of this study should be discussed. First of all, the smaller sample size, due to the limited number of participants; the proof of concept in this study was to demonstrate the possibility to evoke visual potential with smart glasses, anyway, larger dataset should be useful to understand how to improve the measure. In this sense, also the gender distribution and age range should be extended. In fact, as recommended in IFCN recommendations for visual system testing [42] should be useful for each laboratory to establish their own normative values for each decade from the age of 15 years onwards. Another point to discuss is that although the test was monitored closely by an experienced ophthalmologist, it was not possible to monitoring directly the visual fixation. In fact, when the acquisition was conducted with Retimax Advanced® and the TV display, doctors monitored constantly the subjects and urged them to concentrate on their visual task. In the case of the test conducted with the smart glasses, visually monitoring the stability of the fixation was impossible:

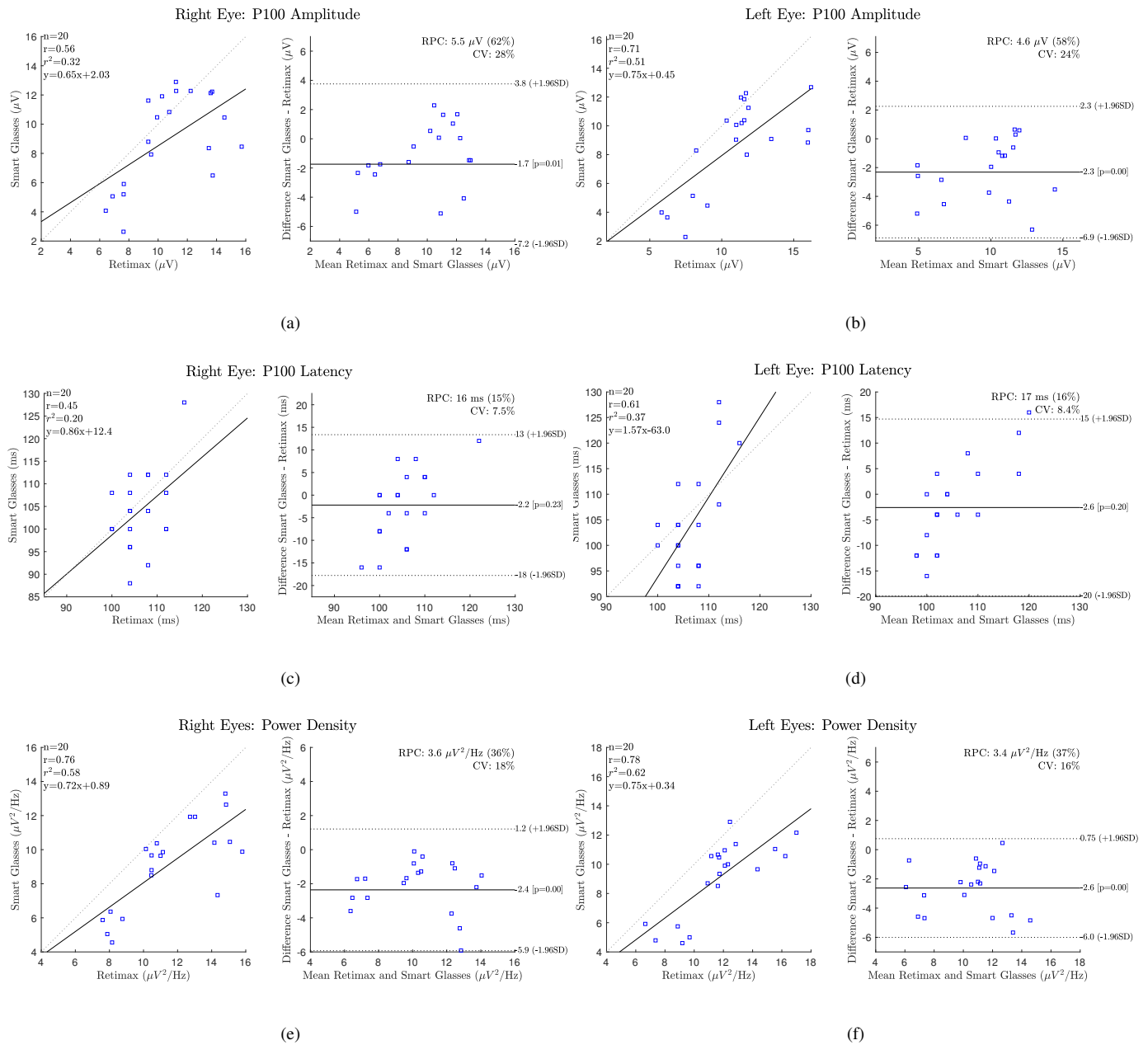


Fig. 5: Scatter plots and Bland-Altman plots obtained in this study for: the P100 Amplitude (a left eye, b right eye), the P100 Latency (c left eye, d right eye) and the Power Density (e left eye, f right eye) data extracted from the signals. As additional information on the correlation are reported: the number of the data points used (n), the Pearson r -value (r), The Pearson r -value squared (r^2), and finally the slope/interception equation. On the other hand, as additional information on the Bland-Altman plots are reported: the reproducibility coefficient (RCP, at 95% confidence level), and coefficient of variation (CV, expressed as standard deviation of mean values in %).

TABLE III: Evaluation of the correlation and the agreement between the two techniques: concordance correlation coefficient (CCC), Pearson correlation coefficient (precision), bias correction factor (χ_b , accuracy) and intraclass correlation coefficient (ICC) was computed at 95% confidence interval.

	Right Eye					Left Eye				
	CCC	Pearson ρ (precision)	χ_b (accuracy)	p-value	ICC	CCC	Pearson ρ (precision)	χ_b (accuracy)	p-value	ICC
Amplitude (μV)										
N75 Amplitude	0.06	0.06	0.95	0.71	-0.04	-0.28	0.30	0.93	0.36	-0.02
P100 Amplitude	0.47	0.56	0.84	0.07	0.13	0.55	0.71	0.77	0.02	0.21
N135 Amplitude	0.38	0.38	0.99	0.89	-0.03	0.46	0.52	0.89	0.33	0.02
N75-P100 Amplitude	0.48	0.52	0.92	0.02	0.04	0.51	0.57	0.89	0.12	0.09
P100-N135 Amplitude	0.51	0.56	0.90	0.17	0.06	0.67	0.74	0.91	0.18	0.07
Latency (ms)										
N75 Time Peak	0.08	0.15	0.52	<0.01	0.46	-0.10	-0.15	0.63	<0.01	0.29
P100 Time Peak	0.34	0.44	0.77	0.34	0.01	0.39	0.61	0.64	0.32	0.02
N135 Time Peak	0.05	0.07	0.74	0.01	0.22	-0.15	-0.16	0.90	0.45	-0.02
N75-P100 Time Peak	0.52	0.68	0.76	0.02	0.22	0.37	0.40	0.91	0.18	0.06
P100-N135 Time Peak	-0.10	-0.15	0.63	<0.01	0.34	-0.09	-0.01	0.84	0.92	-0.05
Frequency Domain ($\mu\text{V}^2/\text{Hz}$)										
Power Density	0.54	0.75	0.70	<0.01	0.28	0.52	0.78	0.66	<0.01	0.34

the eye tested, in fact, was completely covered both by the lens of the glasses and by the 3D printed cover to reduce the external stimuli coming from the background. To mitigate the problem, the operator constantly repeated to maintain the concentration. Moreover, one of the advantage of the head mounted display is the fact that the subject is less prone to distractions because his vision is strictly confined to the mini-display. To overcome this issue an eyeball monitoring system will be integrated in the 3D printed cover. Latencies of smart glasses are slightly different from those recorded with the Retimax Advanced[®], this is probably due to the relatively low sampling frequency of the acquisition board that will be increased in the future to improve time measurements.

In addition to discussed issues, future work needs to include a way to induce flash-VEPs and future studies on intra-subject and inter-session reliability are desirable to proof the clinical usefulness of the proposed device. Above all, the most important work to be done, is the test of our device on pathologic subjects to evaluate the evoked response. This pilot study was conducted on healthy subjects for the device setup and development, but an informal agreement with the hospital will soon lead to more challenging study of abnormal PR-VEP detection.

V. COMPLIANCE WITH ETHICAL STANDARDS

A. Conflict of interest

All authors certify that they have no conflict of interest.

B. Ethical approval

All procedures performed in studies involving human participants were in accordance with the ethical standards of the institutional and/or national research committee and with the 1964 Helsinki Declaration and its later amendments or comparable ethical standards. In addition, this study was approved by the Polytechnic University of Turin as part of a masters thesis [45].

C. Informed consent

Informed consent was obtained from all individual participants included in the study.

REFERENCES

- [1] S. E. Handley and A. C. Liasis, "Multichannel visual evoked potentials in the assessment of visual pathways in children with marked brain abnormalities," *Journal of American Association for Pediatric Ophthalmology and Strabismus*, vol. 21, no. 1, pp. 52–56, 2017.
- [2] M. J. Aminoff and D. S. Goodin, "Visual evoked potentials," *Journal of Clinical Neurophysiology*, vol. 11, no. 5, pp. 493–499, 1994.

- [3] G. D. Dawson, "A summation technique for the detection of small evoked potentials," *Electroencephalography and clinical neurophysiology*, vol. 6, pp. 65–84, 1954.
- [4] C. Wright, G. Harding, and A. Orwin, "The flash and pattern vep as a diagnostic indicator of dementia," *Documenta Ophthalmologica*, vol. 62, no. 1, pp. 89–96, 1986.
- [5] S. P. Neto, L. C. Pinto, and R. M. P. Alvarenga, "The visual evoked potential in idiopathic inflammatory demyelinating diseases," in *Event-Related Potentials and Evoked Potentials*. InTech, 2017.
- [6] G. Stothart, N. Kazanina, R. Näätänen, J. Haworth, and A. Tales, "Early visual evoked potentials and mismatch negativity in alzheimer's disease and mild cognitive impairment," *Journal of Alzheimer's Disease*, vol. 44, no. 2, pp. 397–408, 2015.
- [7] C. Lunghi, M. Berchicci, M. C. Morrone, and F. Di Russo, "Short-term monocular deprivation alters early components of visual evoked potentials," *The Journal of physiology*, vol. 593, no. 19, pp. 4361–4372, 2015.
- [8] C. S. Herrmann, "Human eeg responses to 1–100 hz flicker: resonance phenomena in visual cortex and their potential correlation to cognitive phenomena," *Experimental brain research*, vol. 137, no. 3–4, pp. 346–353, 2001.
- [9] S. T. Fix, J. E. Arruda, F. Andrasik, J. Beach, and K. Groom, "Using visual evoked potentials for the early detection of amnesic mild cognitive impairment: a pilot investigation," *International journal of geriatric psychiatry*, vol. 30, no. 1, pp. 72–79, 2015.
- [10] E. Cerri, C. Fabiani, C. Crisculo, and L. Domenici, "Visual evoked potentials in glaucoma and alzheimers disease," in *Glaucoma*. Springer, 2018, pp. 69–80.
- [11] C. M. Corcoran, A. Stoops, M. Lee, A. Martinez, P. Sehatpour, E. C. Dias, and D. C. Javitt, "Developmental trajectory of mismatch negativity and visual event-related potentials in healthy controls: Implications for neurodevelopmental vs. neurodegenerative models of schizophrenia," *Schizophrenia research*, vol. 191, pp. 101–108, 2018.
- [12] D. Vučinić, "Visual evoked potentials in children and adolescence with neurofibromatosis type 1," *Clinical Neurophysiology*, vol. 126, no. 9, p. e177, 2015.
- [13] P. M. Omland, M. Uglem, K. Hagen, M. Linde, E. Tronvik, and T. Sand, "Visual evoked potentials in migraine: Is the neurophysiological hallmark concept still valid?" *Clinical Neurophysiology*, vol. 127, no. 1, pp. 810–816, 2016.
- [14] P. M. Siper, V. Zemon, J. Gordon, J. George-Jones, S. Lurie, J. Zweifach, T. Tavassoli, A. T. Wang, J. Jamison, J. D. Buxbaum *et al.*, "Rapid and objective assessment of neural function in autism spectrum disorder using transient visual evoked potentials," *PLoS one*, vol. 11, no. 10, p. e0164422, 2016.
- [15] G. Coppola, M. Bracaglia, D. Di Lenola, C. Di Lorenzo, M. Serrao, V. Parisi, A. Di Renzo, F. Martelli, A. Fadda, J. Schoenen *et al.*, "Visual evoked potentials in subgroups of migraine with aura patients," *The journal of headache and pain*, vol. 16, no. 1, p. 92, 2015.
- [16] A. Ambrosini, E. Iezzi, A. Perrotta, A. Kisialiou, A. Nardella, A. Berardelli, F. Pierelli, and J. Schoenen, "Correlation between habituation of visual-evoked potentials and magnetophosphene thresholds in migraine: A case-control study," *Cephalalgia*, vol. 36, no. 3, pp. 258–264, 2016.
- [17] F. Sartucci, T. Bocci, A. Torzini, M. Caleo, E. Giorli, L. Restani, S. Rossi, and L. Maffei, "109. photosensitive epilepsy: Role of corpus callosum in cortical excitability," *Clinical Neurophysiology*, vol. 126, no. 1, p. e25, 2015.
- [18] M. D. Nunez, "Refining understanding of human decision making by testing integrated neurocognitive models of eeg, choice and reaction time," Ph.D. dissertation, University of California, Irvine, 2017.
- [19] J. V. Odom, M. Bach, C. Barber, M. Brigell, M. F. Marmor, A. P. Tormene, G. E. Holder *et al.*, "Visual evoked potentials standard (2004)," *Documenta ophthalmologica*, vol. 108, no. 2, pp. 115–123, 2004.
- [20] J. V. Odom, M. Bach, M. Brigell, G. E. Holder, D. L. McCulloch, A. Mizota, A. P. Tormene, I. S. for Clinical Electrophysiology of Vision *et al.*, "Iseve standard for clinical visual evoked potentials:(2016 update)," *Documenta Ophthalmologica*, vol. 133, no. 1, pp. 1–9, 2016.
- [21] A. R. Whatham, V. Nguyen, Y. Zhu, M. Hennessy, and M. Kalloniatis, "The value of clinical electrophysiology in the assessment of the eye and visual system in the era of advanced imaging," *Clinical and Experimental Optometry*, vol. 97, no. 2, pp. 99–115, 2014.
- [22] D. A. Thompson and A. Liasis, "Visual electrophysiology: how it can help you and your patient," *Taylor and Hoyt's Pediatric Ophthalmology and Strabismus E-Book*, p. 67, 2016.
- [23] R. Sawaya, H. Sawaya, and G. Youssef, "Pattern reversal visual evoked potentials in adults: variability with age," *Clinical and investigative medicine. Medecine clinique et experimentale*, vol. 40, no. 6, pp. E252–E259, 2017.
- [24] A. Halliday, W. McDonald, and J. Mushin, "Delayed visual evoked response in optic neuritis," *The Lancet*, vol. 299, no. 7758, pp. 982–985, 1972.
- [25] C. S. Matsumoto, K. Shinoda, H. Matsumoto, H. Funada, H. Minoda, and A. Mizota, "Liquid crystal display screens as stimulators for visually evoked potentials: flash effect due to delay in luminance changes," *Documenta Ophthalmologica*, vol. 127, no. 2, pp. 103–112, 2013.
- [26] C. S. Matsumoto, K. Shinoda, H. Matsumoto, H. Funada, K. Sasaki, H. Minoda, and A. Mizota, "Comparisons of pattern visually evoked potentials elicited by different response time liquid crystal display screens," *Ophthalmic research*, vol. 51, no. 3, pp. 117–123, 2014.
- [27] B. V. Nagy, S. Gémesi, D. Heller, A. Magyar, Á. Farkas, G. Ábrahám, and B. Varsányi, "Comparison of pattern vep results acquired using crt and tft stimulators in the clinical practice," *Documenta ophthalmologica*, vol. 122, no. 3, pp. 157–162, 2011.
- [28] C. Hanprasertpong, Y. Koizumi, M. Aoyagi, M. Kimura, and T. Yagi, "A head-mounted visual stimulator for neurotological examination," *Auris Nasus Larynx*, vol. 31, no. 4, pp. 379–382, 2004.
- [29] O. Ryohei, I. Masato, M. Shogo, I. Naoaki, and M. Tota, "Development of small device for the brain computer interface with transient vep analysis," in *Region 10 Conference (TENCON), 2016 IEEE*. IEEE, 2016, pp. 3782–3785.
- [30] H. S. Choi, S. H. Im, Y. K. Kim, and S. C. Lee, "Visual evoked potential using head-mounted display versus cathode ray tube: A pilot study," *Annals of rehabilitation medicine*, vol. 40, no. 2, pp. 334–340, 2016.
- [31] C. Italia. (2018) Retimax advanced. [Online]. Available: <http://www.csoitalia.it/en/prodotto/info/31-retimax-advanced>
- [32] C. S. O. CSO, *Retimax Sistema per Elettrofisiologia oculare, Manuale d'uso*, 2013.
- [33] Epson. (2018) Bt-200. [Online]. Available: <https://www.epson.it/products/see-through-mobile-viewer/moverio-bt-200>
- [34] T. Elze, "Achieving precise display timing in visual neuroscience experiments," *Journal of neuroscience methods*, vol. 191, no. 2, pp. 171–179, 2010.
- [35] M. Fox, C. Barber, D. Keating, and A. Perkins, "Comparison of cathode ray tube and liquid crystal display stimulators for use in multifocal vep," *Documenta Ophthalmologica*, vol. 129, no. 2, pp. 115–122, 2014.
- [36] OpenBCI. (2018) Cyton. [Online]. Available: <http://openbci.com/>
- [37] G. H. Klem, H. O. LüEders, H. Jasper, C. Elger *et al.*, "The ten-twenty electrode system of the international federation," *Electroencephalogr Clin Neurophysiol*, vol. 52, no. 3, pp. 3–6, 1999.
- [38] J. Chung, K. H. Jin, J. Kang, and T. G. Kim, "An atypical presentation of functional visual loss: A case report," *Medicine*, vol. 96, no. 41, 2017.
- [39] J. Sanchez-Lopez, C. A. Pedersini, F. Di Russo, N. Cardobi, C. Fonte, V. Varalta, M. Prior, N. Smania, S. Savazzi, and C. A. Marzi, "Visually evoked responses from the blind field of hemianopic patients," *Neuropsychologia*, 2017.
- [40] A. Akay, M. Pehlivan, and G. Çelebi, "A new triggering technique for recording visual evoked potentials," *Biotechnology & Biotechnological Equipment*, vol. 21, no. 2, pp. 250–253, 2007.
- [41] J. L. Steven, *An introduction to the event-related potential technique*. MIT Press, 2005.
- [42] G. E. Holder, G. G. Celesia, Y. Miyake, S. Tobimatsu, R. G. Weleber *et al.*, "International federation of clinical neurophysiology: recommendations for visual system testing," *Clinical Neurophysiology*, vol. 121, no. 9, pp. 1393–1409, 2010.
- [43] A. Souloumian and B. Rivet, "Improved estimation of eeg evoked potentials by jitter compensation and enhancing spatial filters," in *Acoustics, Speech and Signal Processing (ICASSP), 2013 IEEE International Conference on*. IEEE, 2013, pp. 1222–1226.
- [44] J. P. Kelly, F. Darvas, and A. H. Weiss, "Waveform variance and latency jitter of the visual evoked potential in childhood," *Documenta Ophthalmologica*, vol. 128, no. 1, pp. 1–12, 2014.
- [45] R. Terracciano, "Pattern-Reversal Visual Potential Evoked by Android Application on Smart Glasses: prototyping, analysis of the stimulation and acquisition system," Master Degree Thesis in Biomedical Engineering, Politecnico di Torino, 2017.